

# Monitoring molecular motion and structure near defect with STM

Jian-Ru Gong<sup>a,b</sup>, Sheng-Bin Lei<sup>a</sup>, Ge-Bo Pan<sup>a,b</sup>, Li-Jun Wan<sup>a,\*</sup>,  
Qing-Hua Fan<sup>a</sup>, Chun-Li Bai<sup>a,\*</sup>

<sup>a</sup> Key Laboratory of Molecular Nanostructure and Nanotechnology, Institute of Chemistry,  
Chinese Academy of Sciences, Beijing 100080, China

<sup>b</sup> Graduate School of Chinese Academy of Sciences, Beijing, China

Available online 24 November 2004

## Abstract

The diffusion dynamics and enantiomeric structure of the alkyl-substituted isophthalic acid adlayer physisorbed on highly oriented pyrolytic graphite (HOPG) have been investigated in the vicinity of defect by scanning tunneling microscopy (STM). Through molecular motion and reorientation, the defect in the monolayer is filled and an ordered two-dimensional (2D) packing appears. Moreover, an enantiomeric structure is also observed. These findings can be explained by the role of molecular mobility and the cooperation of molecule/molecule and molecule/substrate interactions. The result provides experimental evidences for molecular diffusion and chirality in two dimensions.

© 2004 Elsevier B.V. All rights reserved.

**Keywords:** Isophthalic acid; Diffusion; Defect; STM; Chirality

## 1. Introduction

Since adsorbate diffusion plays an essential role in various surface physical and chemical processes such as heterogeneous catalysis, lubrication, crystal and film growth, gas separation [1], increasing interest has been devoted to understanding of surface diffusion dynamics and developing conceivable microscopical mechanism of atom and molecule motion [2]. From the consideration of isolated adsorbates hopping from site to site on a homogeneous surface, basic mechanism governing surface migration is elucidated [3–5]. However, the in situ information of the organic molecular diffusion in ambient environment is limited, and efforts to study diffusion on a microscopic scale are needed to understand how interactions with the surface and with the neighboring adsorbates influence the way molecules diffuse.

The advent of the scanning tunneling microscopy (STM) has a tremendous impact on atomic and molecular dynam-

ics. STM has the potential to provide high-resolution image, measurement of surface topography and properties on a molecular or even atomic scale due to the much localized nature of the probing, and also, the dynamics of adsorption process and reaction can be studied in space and real time [6]. For example, Stabel et al. studied Ostwald ripening phenomenon in two-dimensional (2D) systems with STM. They have observed the small domain of alkylated anthraquinone and oligothiophene monolayers shrink and finally disappear [7]. Analogous reorientation of molecules and lamellae fragment with respect to the graphite substrate had been documented by earlier work of Rabe and coworkers [8–10]. Fast STM was used to observe the order–disorder transition in monolayers of alkanes at the liquid/graphite interface [11]. Desorption–readsorption or adsorption–desorption process explains the molecular motion in mixed monolayers [12,13].

For the present observation, we concentrate on the surface molecular diffusion process in the vicinity of defect, taking advantaging of 5-(4-hexadecyloxy-benzoyloxy)-isophthalic acid (IA) molecule which related structural characteristics of series of derivatives have been described elsewhere [14].

\* Corresponding authors. Tel.: +86 10 6255 8934; fax: +86 10 6255 8934.  
E-mail addresses: wanlijun@iccas.ac.cn (L.-J. Wan),  
clbai@iccas.ac.cn (C.-L. Bai).

It is found that the IA molecules migrate and reorient to fill the defect in the monolayer. Intriguingly, the observation of an enantiomeric structure is also helpful to explain this dynamic process.

## 2. Experimental

Self-assembly of IA was prepared on freshly cleaved atomically flat surface of HOPG (quality ZYB) by depositing a drop ( $\sim 2 \mu\text{l}$ , less than 1 mM) of IA solution (toluene solvent, HPLC grade, Aldrich). The formation process of the adlayer and molecule diffusion were monitored with a Nanoscope IIIa SPM (Digital Instruments, Santa Barbara, CA) under ambient conditions. STM tips were mechanically cut Pt/Ir wire (90/10). All the STM images were recorded using the constant current mode and without further image processing. The specific tunneling conditions were given in the figure captions.

## 3. Results and discussion

One may expect to study the whole growth process of ordered adlayer after the deposition of IA onto the substrate. However, the initial adsorption process is too fast to be observed by STM for this system. The most likely mechanism of the initial adsorption [15] involves: (i) the equilibration of critical-size nuclei with an adsorbed monomer population which in turn is equilibrated with the liquid phase, and (ii) growth of the critical nuclei by surface diffusion of the adsorbed monomer. Although molecular defects at the initial stage are apparent, no dynamic information at the initial stage of the monolayer formation has been achieved. The defect filling process at the next stage is relatively a slow dynamic process which can be studied by STM.

Fig. 1 is a series of time-dependent STM images showing the dynamic process recorded in the vicinity of defect. Shortly after depositing IA molecules on HOPG surface, a relatively disordered adlayer with a defect (circled in Fig. 1a, the time of the first image is arbitrarily set to zero,  $t = 0 \text{ min}$ ) on the upper right of the scanned area is observed. The bright bands in the image as shown in Fig. 1a correspond to the aromatic cores of IA molecules, and the dark stripes correspond to the close-packed alkane chains. In Fig. 1b ( $t = 20 \text{ min}$ ) it can be seen that molecular diffusion onto the free space induces width of the defect size smaller. The fuzzy image near the defect area might be ascribed to high mobility of the IA molecules due to the absence of strong interactions. Subsequently, several segments of lamellae are observed in Fig. 1c ( $t = 25 \text{ min}$ ). The vacancy is almost filled up to form a continuous adlayer. With increasing time (Fig. 1d), the parallel lamellae show ordered packing. Simultaneously most of the molecules in the field of view are ordered into a 2D layer by steric crowding. Fig. 2 gives a model for the molecular deposition process in the

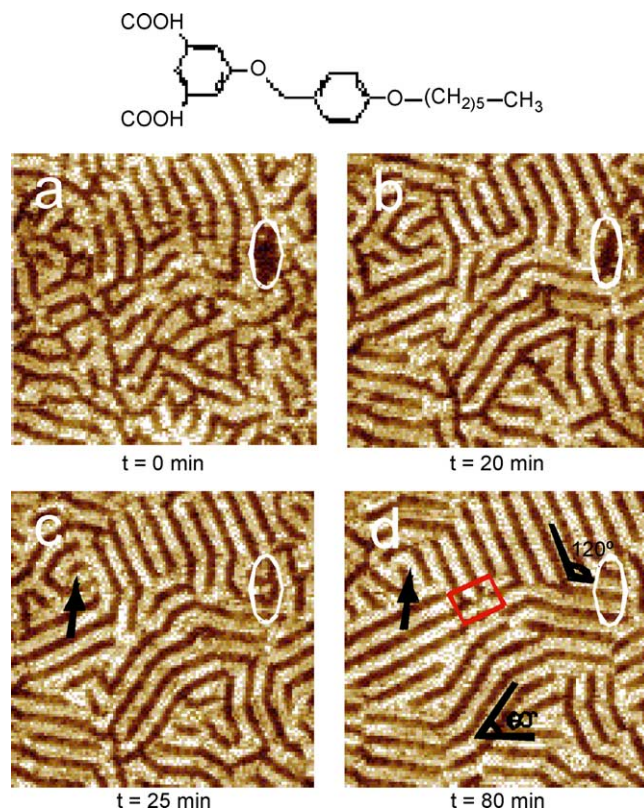


Fig. 1. Series of STM images of a  $75 \text{ nm} \times 75 \text{ nm}$  region of IA illustrating the dynamic process in the vicinity of the defect recorded with  $V = 821 \text{ mV}$  and  $I = 762 \text{ pA}$ . The black arrow in (c) and (d) demonstrate the molecular reorientation. The encircled part indicates the defect area.

defect area of Fig. 1, corresponding to a surface concentration of about  $4.5 \times 10^{15} \text{ molecules/cm}^2$ , which is slightly smaller than that found for the close-packed arrangement. The net filling rate could be defined to be about 23 molecules/h in the recording interval of 80 min, i.e., during 1 h, 23 molecules come into the defect area.

There are two possibilities for the disappearance of the defects: (1) the defects are formed by incomplete coverage of molecules, that is, there are few molecules in the vacant area. The disappearance of the defects is caused by diffusion of molecules on surface. Not surprisingly, there is more free volume in the defect area, typically a region with a lower stability and enhanced dynamics. The molecules will migrate or reorientate to reduce the free volume and thereby minimize the free energy. (2) The defect area is occupied by randomly adsorbed molecules. The inability to image the molecules in the position of the defect suggests the less-favorable molecular packing or high mobility. The disappearance of vacancy is caused by reorientation or migration of the molecules. Since the molecular density of a disordered area may lower than that of an ordered lamella, the defect is more likely to be caused by incomplete molecular coverage, and its disappearance can be explained as a consequence of the space-filling principle.

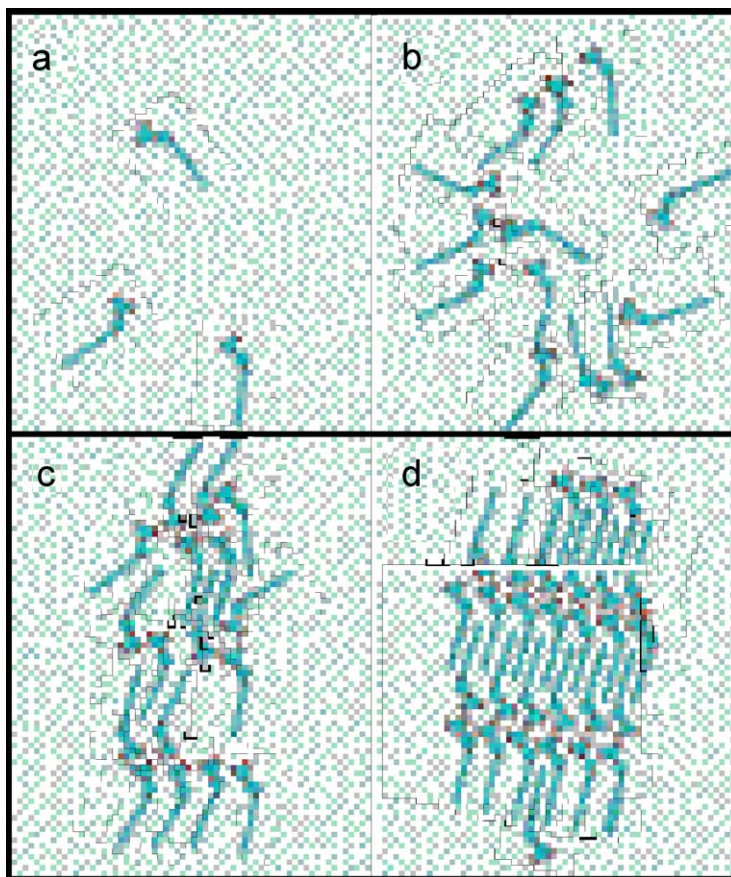


Fig. 2. The model for the molecular deposition process in the defect area of Fig. 1. About 30 molecules fill into the defect area in the recording interval of 80 min.

From Fig. 1d domains orientated with  $60^\circ$  or  $120^\circ$  can be observed, this can be attributed to the commensuration of alkyl chains with the three-fold rotational symmetry of the graphite lattice. But the emergence of  $90^\circ$  orientate domains (as can be observed in the center of Fig. 1d) is somewhat amazing. In addition, the lamellae indicated by the black arrow in Fig. 1c and d are observed to rotate by  $90^\circ$  with respect to the initial orientation. In order to make clear the orientation of the domains and the reorientation process, high resolution images have been acquired on the  $90^\circ$  orientate domain boundary.

A high resolution STM image (Fig. 3a) from the area marked by the red rectangle in Fig. 1d reveals an adlayer with  $90^\circ$ -rotated lamellae. The orientation of the underlying HOPG surface is presented as an inset in Fig. 3a. From the STM image, an enantiomeric structure in IA adlayer is clearly resolved, and the emergence of the enantiomeric structure is illustrated in Fig. 3b. Fig. 3c shows STM images for two enantiomeric domains on IA adlayer with submolecular resolution. The corresponding molecular model is illustrated on the image. The bright bands and dark stripes are alternating over the substrate. The bright band consists of regular dots with a diameter of  $0.5 \pm 0.05$  nm. Each bright spot is assumed to be a benzene ring in the aromatic core. Owing to

the large electronic density of benzene, the contrast of this part is higher than the alkyl chains. Besides the bright dots, the darker regions in the image correspond to the alkyl groups of the molecules, with the chain-width 0.45 nm, indicating a flat-lying molecular geometry with alkyl chains parallel to the substrate [16]. For the existence of carboxyl groups, hydrogen bonds can be formed among IA molecules. In the image, all the molecules are packed head (carboxyl)-to-head. A unit cell outlined in Fig. 3c contains two molecules with parameters  $a = 4.5 \pm 0.1$  nm,  $b = 1.2 \pm 0.1$  nm,  $\alpha = 87.2 \pm 2^\circ$ . The image indicates that the alkyl chains of the molecules are interdigitated over the full length of the chains in the lamellae. By the interdigitation of the alkyl chains, a close-packed arrangement of IA is realized. This space filling properties of alkyl chains and planar aromatic cores minimize the free space within the monolayer on the graphite surface, and result in a maximum of the intermolecular and molecule/graphite interactions. In this way, a stable monolayer with a sufficiently low molecular lateral mobility is assembled [17]. Note that hydrogen bondings between the carboxyl groups also contribute to the stability of the assembly.

Various studies have shown that substrate surface can be used as a symmetry breaking agent to induce enantiomorphic ordering in assemblies produced even by depositing achiral

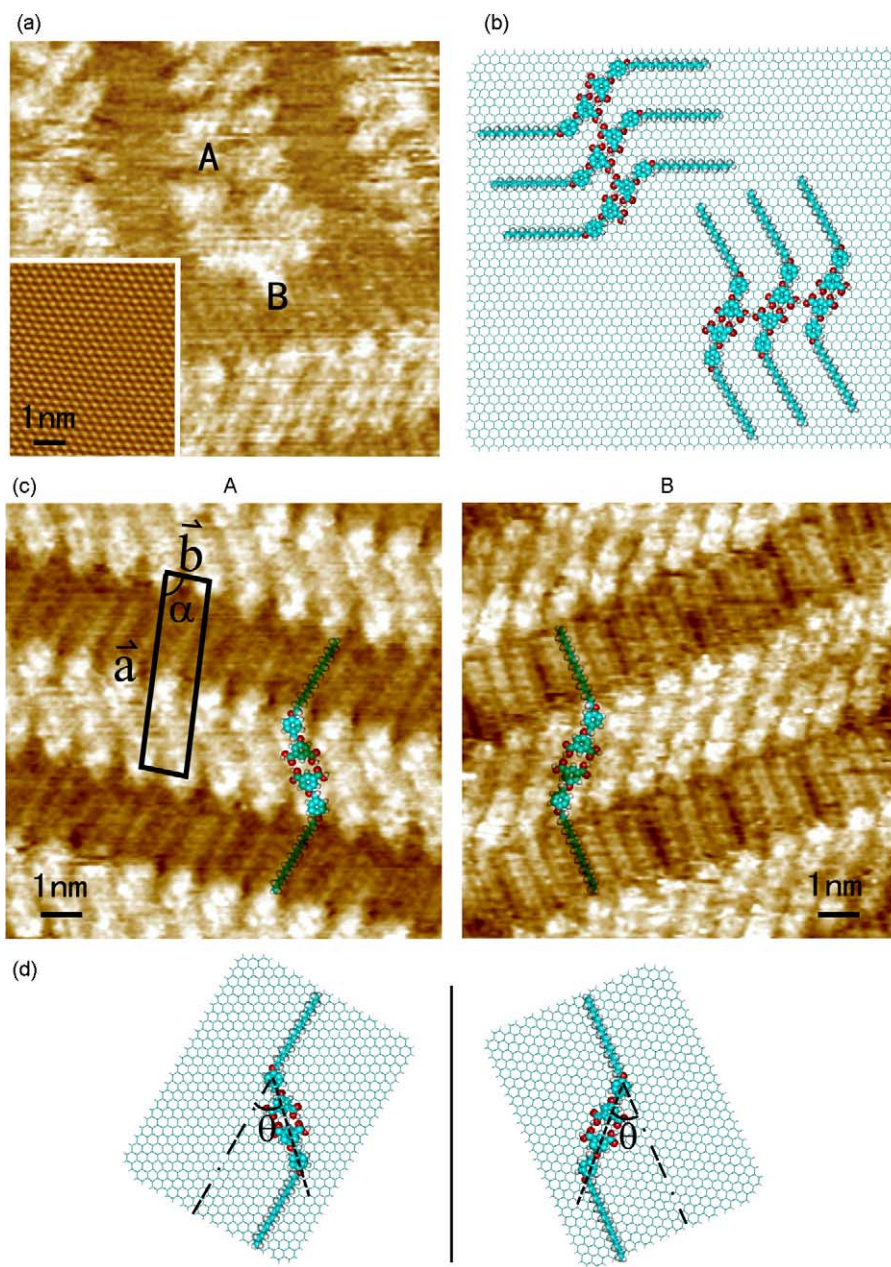


Fig. 3. (a) A zoomed-in image in Fig. 1 marked by the red rectangle. The inset in (a) is an underlying graphite substrate. A and B indicate two chiral areas. Recorded with  $V=757$  mV,  $I=203$  pA. (b) The molecular model of Fig. 2a. (c) High resolution images of two chiral areas A recorded with  $V=569$  mV,  $I=163$  pA and B recorded with  $V=650$  mV,  $I=374$  pA. The unit cell as shown in Fig. 2c composes two molecules with parameters  $a=4.5 \pm 0.1$  nm,  $b=1.2 \pm 0.1$  nm,  $\alpha=87.2 \pm 2^\circ$ . (d) Corresponding molecular models with chiral structures.  $\theta$  is the angle between the lamella axis and the graphite reference axis. The black vertical line is a reflection plane emphasizing that these two conformers are mirror images of one another.

molecules [18–23]. When IA adsorbs onto a surface, rotation of the C–C bond connecting the alkyl “tail” to the isophthalic acid “head” becomes strongly hindered. This rotational barrier imparts a new chiral center to the molecule. As a result, IA molecules exhibit mirror image on the surface as shown in Fig. 3c. A model for the molecular chiral structures is depicted in Fig. 3d. This enantiomorphism is expressed by the orientation of the lamella axes with respect to the graphite lattice: the angle  $\theta$  between a lamella axis (any line parallel to a row formed by aromatic groups) and a graphite refer-

ence axis, which is parallel to the alkyl chains, takes a value of  $-45^\circ$  and  $+45^\circ$  for molecules in domains A and B, respectively. Note that the chirality of a domain is also expressed without making reference to the graphite surface underneath. However, for this system, comparison of the monolayer orientation with the underlying graphite surface provides an elegant means for analysis.

As discussed above, the  $90^\circ$  orientation of the domains is revealed to be caused by enantiomorphic adsorption of IA, this indicates that the  $90^\circ$  reorientation process observed

in Fig. 1 must involve desorption–adsorption process of molecules, since  $90^\circ$  orientation cannot be realized by simple molecular rotation on the surface.

The cooperation of molecule/molecule and molecule/substrate interactions contributes to the formation of the ordered self-assembled structure, which could be inferred from the intermolecular hydrogen bonding and enantiomeric domains in the monolayer. The diffusion and rotation of molecules in the vicinity of defect allow the reorientation, desorption–adsorption process also involves in the ordering process as mentioned above. According to Ostwald ripening [24], the lamella fragments and small domains incorporate the larger structure to reduce the free volume and thereby minimize the free energy. When eventually thermodynamic equilibrium is attained, though the aleatoric thermal mobility persists, there is a uniform adsorbate distribution on the surface and no further net surface mass transport takes place, as could be seen from the stable monolayer in Fig. 1d. After obtaining the last image, we enlarged the scan area and no apparent difference has been seen for the center area from the surrounding part. So we could infer that the influence of scanning tip is neglectable for the current system.

#### 4. Conclusions

In summary, the dynamic process of surface molecular diffusion in the vicinity of defect was observed on HOPG by STM. Through molecular motion and reorientation, the defect in the monolayer was filled and well-ordered 2D packing was formed. Also, an enantiomeric structure was observed. The cooperation of molecule/molecule and molecule/substrate interactions contributes to the formation of the ordered self-assembling structure. The present results provide direct and preliminary evidence for molecular adsorption and diffusion near defect and could be helpful to understand the dynamic mechanism of surface adsorption processes.

#### Acknowledgements

This work was supported by National Natural Science Foundation of China (Nos. 20025308, 20303023 and 20177025), National Key Project on Basic Research (Grants

G2000077501), the Chinese Academy of Sciences, and the Outstanding Innovation Group Foundation (20121301).

#### References

- [1] A.A. Levchenko, B.P. Argo, R. Vidu, R.V. Talroze, P. Stroeve, *Langmuir* 18 (2002) 8464.
- [2] F. Niet, C. Uebing, V. Pereyra, *Surf. Sci.* 416 (1998) 152.
- [3] T. Mitsui, M.K. Rose, E. Fomin, D.F. Ogletree, M. Salmeron, *Science* 297 (2002) 1850.
- [4] H. Xu, I. Harrison, *J. Phys. Chem. B* 103 (1999) 11233.
- [5] N. Lin, A. Dmitriev, J. Weckesser, J.V. Barth, K. Kern, *Angew. Chem. Int. Ed.* 41 (2002) 4779.
- [6] G.S. McCarty, P.S. Weiss, *Chem. Rev.* 99 (1999) 1665.
- [7] A. Stabel, R. Heinz, F.C. De Schryver, J.P. Rabe, *J. Phys. Chem.* 99 (1995) 505.
- [8] A. Stabel, R. Heinz, J.P. Rabe, G. Wegner, F.C. De Schryver, D. Corens, W. Dehaen, C. Süling, *J. Phys. Chem.* 99 (1995) 8690.
- [9] T.L. Liu, J.P. Parakka, M.P. Cava, Y.T. Kim, *Langmuir* 11 (1995) 4205.
- [10] R. Heinz, J.P. Rabe, W.-V. Meister, S. Hoffmann, *Thin Solid Films* 264 (1995) 246.
- [11] Askadskaya, J.P. Rabe, *Phys. Rev. Lett.* 69 (1992) 1395.
- [12] N. Elbel, W. Roth, E. Günther, H. von Seggern, *Surf. Sci.* 303 (1994) 424.
- [13] M. Hibino, A. Sumi, I. Hatta, *Thin Solid Films* 273 (1996) 272.
- [14] J.-R. Gong, S.-B. Lei, L.-J. Wan, G.J. Deng, Q.-H. Fan, C.-L. Bai, *Chem. Mater.* 15 (16) (2003) 3098.
- [15] G.M. Pound, M.T. Simnad, L. Yang, *J. Chem. Phys.* 22 (1954) 1215.
- [16] G.C. McGonigal, R.H. Bernhardt, D.J. Thomson, *Appl. Phys. Lett.* 57 (1990) 28.
- [17] P. Vanoppen, P.C.M. Grim, M. Rücker, S. De Feyter, G. Moessner, S. Valiyaveetil, K. Müllen, F.C. De Schryver, *J. Phys. Chem.* 100 (1996) 19636.
- [18] M. Böhlinger, K. Morgenstern, W.-D. Schneider, R. Berndt, *Angew. Chem. Int. Ed.* 38 (1999) 821.
- [19] M.O. Lorenzo, C.J. Baddeley, C. Muryn, R. Raval, *Nature* 404 (2000) 376.
- [20] J. Weckesser, A.D. Vita, J.V. Barth, C. Cai, K. Kern, *Phys. Rev. Lett.* 87 (2001) 096101.
- [21] A. Kühnle, T.R. Linderoth, B. Hammer, F. Besenbacher, *Nature* 415 (2002) 891.
- [22] J.V. Barth, J. Weckesser, G. Trimarchi, M. Vladimirova, A.D. Vita, C. Cai, H. Brune, P. Günter, K.J. Kern, *J. Am. Chem. Soc.* 124 (2002) 7991.
- [23] S. De Feyter, P.C. Grim, M. Rücker, P. Vanoppen, C. Meiners, M. Sieffert, S. Valiyaveetil, K. Müllen, F.C. De Schryver, *Angew. Chem. Int. Ed.* 37 (1998) 1223.
- [24] S. De Feyter, A. Gesquière, M.M. Abdel-Mottaleb, P.C.M. Grim, F.C. De Schryver, *Acc. Chem. Res.* 33 (2000) 520.